Demonstration of boron arsenide heterojunctions: A radiation hard wide band gap semiconductor device

Y. Gong,[1,a)] M. Tapajna,[1] S. Bakalova,[1] Y. Zhang,[2] J. H. Edgar,[2] Y. Zhang,[3] M. Dudley,[3] M. Hopkins,[4] and M. Kuball[1]
[1]H.H. Wills Physics Laboratory, University of Bristol, Bristol BS8 1TL, United Kingdom
[2]Department of Chemical Engineering, Kansas State University, Manhattan, Kansas 66506, USA
[3]Department of Materials Science and Engineering, SUNY, Stony Brook, New York 11794, USA
[4]Department of Electronic and Electrical Engineering, University of Bath, Bath BA2 7AY, United Kingdom

(Received 13 January 2010; accepted 12 May 2010; published online 4 June 2010)

$B_{12}As_2$/SiC *pn* heterojunction diodes based on the radiation-hard $B_{12}As_2$ deposited on (0001) *n*-type 4H–SiC via chemical vapor deposition were demonstrated. The diodes exhibit good rectifying behavior with an ideality factor of 1.8 and a leakage current as low as 9.4×10^{-6} A/cm^2. Capacitance-voltage measurements using a two-frequency technique showed a hole concentration of $\sim 1.8-2.0 \times 10^{17}$ cm^{-3} in $B_{12}As_2$ with a slight increase near the interface due to the presence of an interfacial layer to accommodate lattice mismatch. Band offsets between the $B_{12}As_2$ and SiC were estimated to be ~ 1.06 eV and 1.12 eV for conduction band and valance band, respectively. © *2010 American Institute of Physics*. [doi:10.1063/1.3443712]

Icosahedral boron arsenide ($B_{12}As_2$) is a wide band gap boron-rich semiconductor ($E_g \approx 3.20$ eV at room temperature[1]). Its structure is based on 12-boron-atom icosahedra residing at the lattice points of a rhombohedral unit cell, with an As–As chain lying along its [111] axis (the body diagonal) (Refs. 2 and 3) [Fig. 1(a)]. The boron atoms in the icosahedra are bonded by so-called three-centered bonds, i.e., a pair of electrons is shared among three boron atoms. As a consequence of this unique structure and bonding, $B_{12}As_2$ has extraordinary radiation tolerance via self-healing mechanisms. In addition, it has a high melting temperature, and excellent mechanical properties, making $B_{12}As_2$ highly attractive for applications under harsh conditions. Further details on the material properties of $B_{12}As_2$ can be found in Refs. 1–7, and reference therein.

A key potential application of $B_{12}As_2$ is for compact solid-state thermal neutron detectors because ^{10}B has one of the highest thermal neutron (0.0259 eV) capture cross-sections, ~3840 b of all elements.[8] When thermal neutrons are absorbed by ^{10}B, energetic ^{7}Li and ^{4}He ions form, predominantly via $^{10}\mathrm{B}+n \rightarrow {}^{7}\mathrm{Li}(0.84\ \mathrm{MeV})+{}^{4}\mathrm{He}(1.47\ \mathrm{MeV})$, and electron-hole pairs are created as the ^{7}Li or ^{4}He ions passing through the material. Compared with the present mature neutron detection technology employing gas-filled, proportional counters, or doped scintillating plastic fibers, solid-state neutron detectors would have reduced size and weight features that are beneficial for applications in portable devices or space. A further potential application is for betavoltaics, converting nuclear energy into electrical power, for small-scale long-lifetime batteries, e.g., remote sensors and peacemakers, where present materials are susceptible to radiation damage.[9] Despite this great potential, no success has been achieved in fabricating $B_{12}As_2$ based devices up to date, presumably due to the difficulty in growing high crystalline quality $B_{12}As_2$. In this paper, we report the fabrication of $B_{12}As_2$/SiC *pn* diodes, and present a detailed analysis of their electrical properties.

a)Electronic mail: yinyan.gong@bristol.ac.uk.

Vertical heterojunction diodes were fabricated by epitaxially depositing $B_{12}As_2$ on 300 μm thick silicon-face (0001) *n*-type 4H–SiC ($n \approx 10^{18}$ cm^{-3}) using chemical vapor deposition (CVD) at 1350 °C under a constant total pressure of 100 Torr using 1% B_2H_6 in H_2 and 2% AsH_3 in H_2 in hydrogen atmosphere. More details on the growth and its microstructure can be found in Refs. 5 and 7. Ohmic contacts to the $B_{12}As_2$ were formed by depositing 50 nm Cr and 100 nm Pt using e-beam evaporator through a shadow mask, followed by annealing at 600 °C for 10 min in an Ar ambient.[10] Ohmic contacts to the *n*-type SiC were achieved by sputtering 100 nm Ni through a shadow mask, followed

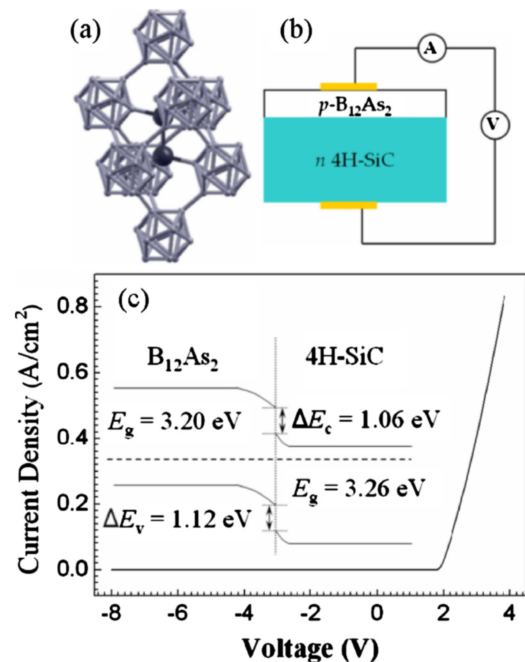

FIG. 1. (Color online) (a) Rhombohedral unit cell of $B_{12}As_2$, (b) schematic diode geometry, and (c) *I-V* curve of a representative $B_{12}As_2$/SiC *pn*-heterojunction diode with inset showing a schematic representation of energy band diagram.

 © 2010 American Institute of Physics

Downloaded 24 Jul 2010 to 129.130.103.82. Redistribution subject to AIP license or copyright; see http://apl.aip.org/apl/copyright.jsp

by annealing at 950 °C for 2 min in an Ar ambient. Figure 1(b) shows a schematic of a $B_{12}As_2/SiC$ heterojunction diode. The electrical properties of the diodes were characterized by current-voltage (*I-V*) and capacitance-voltage (*C-V*) measurements using a Keithley 4200 semiconductor characterization system. High resolution transmission electron microscopy (HRTEM) observations were carried out using a 200 keV JEOL 2100 system at the Center for Functional Nanomaterials, Brookhaven National Laboratory.

Figure 1(c) shows the *I-V* characteristics of a $B_{12}As_2/SiC$ heterojunction with a film thickness of 4.3 μm, exhibiting excellent rectifying behavior with an I_F/I_R value as high as 4.14×10^3 at 3 V indicating the formation of a *pn* diode (I_F and I_R stand for forward and reverse current, respectively). Hall-effect measurements on $B_{12}As_2$ films (not shown here) and previous work[3] showed that undoped $B_{12}As_2$ is usually *p*-type, and therefore when it is grown epitaxially on *n*-type SiC, holes will diffuse from $B_{12}As_2$ into 4H–SiC while electrons will diffuse from 4H–SiC to $B_{12}As_2$, resulting in the formation of a depletion region and a total electrostatic potential across the junction as in a standard *pn* junction [inset of Fig. 1(c)]. Details on the determination of the band offsets will be discussed in the following section. We note that *n*-doping of $B_{12}As_2$ has not been demonstrated to date, i.e., therefore, the approach of a heterojunction is taken here.

An ideality factor, *n*, of ~1.8 was extracted from the *I-V* curve under forward-biased conditions of the studied $B_{12}As_2/SiC$ *pn* diode, implying that in part recombination current may contribute to the electrical characteristics of the diode. The leakage current is $\sim9.4\times10^{-6}$ A/cm^2 under a reverse bias of 0.4 V, which however, is three orders of magnitude higher than for typical single-crystalline 4H–SiC *pn* junction diodes.[11] This higher leakage current can be attributed, at least partially, to structural defects due to the heteroepitaxial growth of $B_{12}As_2$ on 4H–SiC. $B_{12}As_2$ on 4H–SiC exhibits twin boundaries [Fig. 2(a)] perpendicular to the interface of the heterojunction. While each grain is highly crystalline [Fig. 2(b)], they are present in two distinct orientations and the boundaries between them can serve as leakage pathways in the *pn* junction. The higher density of twin boundaries is consistent with the leakage current magnitude observed. Details on the atomic structure of twin boundaries in $B_{12}As_2$ can be found in Refs. 5 and 7. We further note the presence of a thin, relatively disordered transition layer located between the film and the substrate [Fig. 2(a)]. Trap states associated to these and other structural defects will contribute to recombination currents in the *pn*-junction. Despite the presence of these structural imperfections, good device rectifying behavior is achieved. Only a reduction in their density by recent growth improvements[7] has made this possible. It is expected that the diode performance can be further improved by reducing structural defects even further. For example depositing $B_{12}As_2$ onto *m*-plane 15R–SiC substrates can eliminate twin boundaries,[4] although *n*-type 15R–SiC is presently not available commercially.

The *C-V* measurements were performed on the $B_{12}As_2/SiC$ diode from 5 to 500 kHz. The measured capacitance decreases with increasing frequency, implying that both series resistance and leakage current needed to be considered in the analysis.[12–14] A three-element circuit model representing the diode is shown in the inset of Fig. 3, with *C*

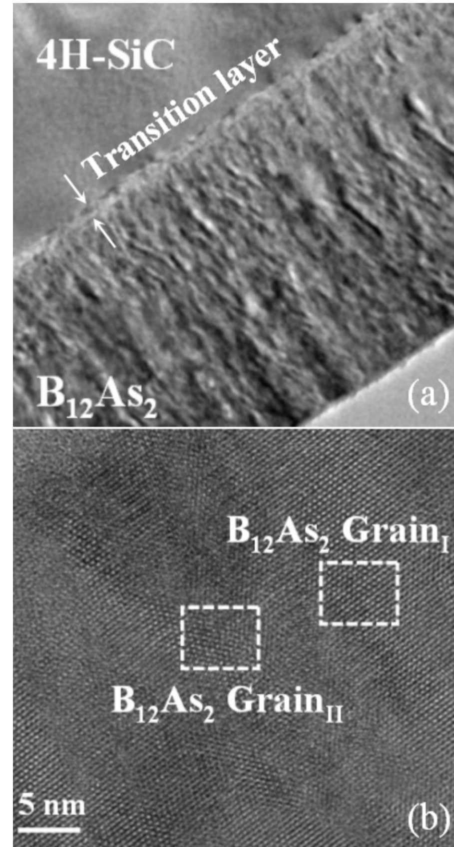

FIG. 2. (a) Cross-sectional TEM micrograph of $B_{12}As_2$/4H–SiC heterojunction, revealing twin boundaries perpendicular to the interface. Also apparent is a transition layer between the $B_{12}As_2$ and the SiC substrate. (b) HRTEM micrograph of $B_{12}As_2$ grains in different orientations, labeled by the subscript I and II, respectively.

is the actual frequency-independent diode capacitance, R_s is the series resistance, and R_p is the effective diode resistance due to leakage current. From a single measurement of impedance, only two of these three parameters may be determined. To consider both the series resistance and the leakage current, a two-frequency *C-V* technique by Yang and Hu[14] was used to extract *C* using the following expression:

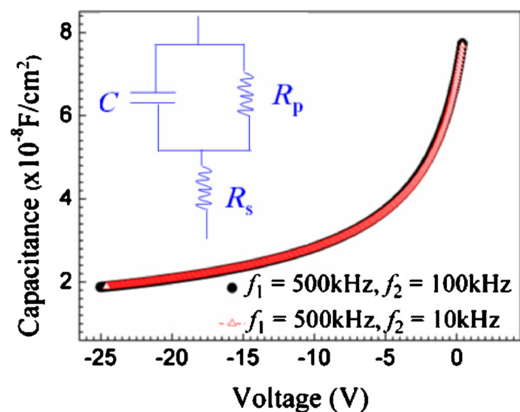

FIG. 3. (Color online) *C-V* data analyzed using the two-frequency technique, considering the simultaneous presence of both series resistance and leakage current, with inset showing the equivalent circuit model for the *pn* diode.

Downloaded 24 Jul 2010 to 129.130.103.82. Redistribution subject to AIP license or copyright; see http://apl.aip.org/apl/copyright.jsp

$$C=\frac{f_1^2C_1(1+D_1^2)-f_2^2C_2(1+D_2^2)}{f_1^2-f_2^2}, \quad (1)$$

where C_1 and C_2 are the capacitance measured at the frequency f_1 and f_2, respectively, D_1 $(=G_1/2\pi f_1C_1)$ and D_2 $(=G_2/2\pi C_2)$ are the dissipation at the frequency f_1 and f_2, respectively, G_1 and G_2 are the diode conductance at the frequency f_1 and f_2, respectively. Figure 3 shows the determined diode capacitance with $f_1=500$ kHz and $f_2=100$ kHz, and $f_1=500$ kHz and $f_2=10$ kHz, with both data sets in good agreement, illustrating that the technique is applicable to the *C-V* measurement on $B_{12}As_2$/SiC *pn* diode.

Under the assumption of abrupt junction, the hole concentration in $B_{12}As_2$ film is given by

$$N_A(W)=2\left[q\varepsilon_sA^2\frac{d(1/C^2)}{dV}\right]^{-1}, \quad (2)$$

where q is the electron charge, ε_s [≈7.15 (Ref. 1)] is the permittivity of $B_{12}As_2$, A is the junction area, and W $(=\varepsilon_sA/C)$ is depletion layer width.[13] With the free hole concentration in $B_{12}As_2$ typically much lower than the free electron concentration in *n*-type 4H–SiC substrate, for simplicity, we neglect the spreading of space-charge region into the substrate. The determined free hole concentration in the $B_{12}As_2$ film is in the range of $\sim 1.8-2.0\times 10^{17}$ cm^{-3}, with a slightly higher density near the interface, which might be due to the existence of the interfacial layer between $B_{12}As_2$ and the 4H–SiC.

The built-in potential of the diodes, extracted by extrapolating $1/C^2$ versus V as $1/C^2$ to zero, is ~1.89 V. According to Anderson's energy band model,[15] the band offsets of a heterojunction can be estimated using the following expression: $\Delta E_c=qV_{bi}-E_{g1}+(\delta_{v1}+\delta_{c2})$, where δ_v (δ_c) is the separation between Fermi level and valence band (conduction band), and subscript 1 and 2 referred to $B_{12}As_2$ and SiC, respectively. Given the energy band gap of 4H–SiC (~3.26 eV),[16] the estimated band offsets are ~1.06 eV and 1.12 eV for conduction band and valance band, respectively [inset of Fig. 1(c)]. Although this can only serve as rough estimation, the knowledge of band alignment is important for the future work on $B_{12}As_2$ device applications.

In conclusion, we have successfully demonstrated $B_{12}As_2$/4H–SiC *pn* heterojunction diodes by depositing $B_{12}As_2$ on *n*-type 4H–SiC by CVD. Electrical properties of the diodes were characterized by *I-V* and *C-V* measurements. A good rectifying behavior was observed which confirms the formation of *pn* heterojunction diode. A two-frequency technique was employed to analyze *C-V* data, and the obtained free hole concentration in the $B_{12}As_2$ film is $\sim 1.8-2.0\times 10^{17}$ cm^{-3}, and the band offsets are ~1.06 eV and 1.12 eV for conduction band and valance band, respectively.

The authors gratefully acknowledge the support by the Engineering and Physical Science Research Council (EPSRC) under Grant No. EP/D075033/1, by the National Science Foundation Materials World Network Program under Grant No. 0602875 under the NSF-EPSRC Joint Materials Program, and by the U.S. Department of Energy under Contract No. DE-AC02-98CH10886.

[1]S. Bakalova, Y. Gong, C. Cobet, N. Esser, Y. Zhang, J. H. Edgar, Y. Zhang, M. Duddley, and M. Kuball, Phys. Rev. B **81**, 075114 (2010).
[2]D. Emin, Phys. Today **40**(1), 55 (1987).
[3]D. Emin, J. Solid State Chem. **177**, 1619 (2004).
[4]H. Chen, G. Wang, M. Dudley, Z. Xu, J. H. Edgar, T. Batten, M. Kuball, L. Zhang, and Y. Zhu, Appl. Phys. Lett. **92**, 231917 (2008).
[5]H. Chen, G. Wang, M. Dudley, L. Zhang, L. Wu, Y. Zhu, Z. Xu, J. H. Edgar, and M. Kuball, J. Appl. Phys. **103**, 123508 (2008).
[6]D. Emin, J. Solid State Chem. **179**, 2791 (2006); G. A. Slack, T. M. McNelly, and E. A. Taft, J. Phys. Chem. Solids **44**, 1009 (1983).
[7]R. Nagarajan, Z. Xu, J. H. Edgar, F. Baig, J. Chaudhuri, Z. Rek, E. A. Payzant, H. M. Meyer, J. Pomeroy, and M. Kuball, J. Cryst. Growth **273**, 431 (2005).
[8]V. F. Sears, Neutron News **3**, 26 (1992).
[9]B. Danilchenko, A. Kudnyk, L. Shpinar, D. Poplavskyy, S. E. Zelensky, K. W. J. Barnham, and N. J. Ekins-Daukes, Sol. Energy Mater. Sol. Cells **92**, 1336 (2008); P. Rappaport, Phys. Rev. **93**, 246 (1954); R. L. Statler, Radiat. Eff. Defects Solids **4**, 305 (1970).
[10]S. H. Wang, E. M. Lysczek, B. Liu, S. E. Mohney, Z. Xu, R. Nagarajan, and J. H. Edgar, Appl. Phys. Lett. **87**, 042103 (2005).
[11]F. Moscatelli, A. Scorzoni, A. Poggi, M. Bruzzi, S. Sciortino, S. Lagomarsino, G. Wagner, I. Mandic, and R. Nipoti, IEEE Trans. Nucl. Sci. **53**, 1557 (2006).
[12]G. I. Roberts and C. R. Crowell, J. Appl. Phys. **41**, 1767 (1970); Y. Wang, K. P. Cheung, R. Choi, and B. H. Lee, IEEE Trans. Electron Devices **55**, 2429 (2008).
[13]D. K. Schroder, *Semiconductor Material and Device Characterization*, 3rd ed. (Wiley, New York, 2006).
[14]K. J. Yang and C. Hu, IEEE Trans. Electron Devices **46**, 1500 (1999).
[15]R. L. Anderson, Solid-State Electron. **5**, 341 (1962); J. P. Donnelly and A. G. Milines, IEEE Trans. Electron Devices **14**, 63 (1967).
[16]C. Persson and U. Lindefelt, Phys. Rev. B **54**, 10257 (1996).

Downloaded 24 Jul 2010 to 129.130.103.82. Redistribution subject to AIP license or copyright; see http://apl.aip.org/apl/copyright.jsp